RSC Advances

PAPER

View Article Online
View Journal | View Issue

Cite this: *RSC Adv.*, 2014, **4**, 42965

Monodisperse, nanoporous ceria microspheres embedded with Pt nanoparticles: general facile synthesis and catalytic application†

Lin Zhou,[a] Xiaoxiao Li,[b] Yong Wang,[a] Mei Hong,*[a] Yongye Liang*[b] and Jing Zhao*[ac]

Received 10th June 2014
Accepted 12th August 2014

DOI: 10.1039/c4ra08423c

www.rsc.org/advances

A monodisperse Pt/ceria hybrid with controlled nanoporous structure was fabricated with the aid of poly(glycidyl methacrylate-*co*-ethylene glycol dimethacrylate) microspheres as a hard template. Functional groups on the polymer microspheres interacted with Pt species and then cerium precursors were impregnated into the microsphere pores through a sol–gel method. Porous ceria microspheres embedded with uniform and fine Pt nanoparticles formed after removal of the polymer templates by calcination. The hierarchical Pt/ceria hybrid possesses catalytic activity, excellent stability and ease of recyclability. For example, a highly efficient catalytic reduction of 4-nitrophenol (4-NP) with sodium borohydride was accomplished. This facile and general synthetic method could be extended to other novel metal/oxide hybrid combinations.

Introduction

The catalytic properties of a supported metal system are found to be closely related to the type and morphology of support involved.[1] As supports, metal oxides can efficiently prevent agglomeration and deactivation of the dispersed metal nanoparticles.[2] Ceria (CeO_2) has been applied as a support to construct catalysts for a wide variety of reactions, such as CO oxidation,[3] hydrogenation[4] and water–gas shift.[5] The advantages of ceria in catalysis can be attributed to its intrinsic features, such as abundant oxygen vacancy defects, peerless oxygen storing/releasing capabilities, and easy shuttle between the III and IV oxidation states.[6] In particular, noble metal/ceria-based catalysts have long been known to exhibit strong metal–support interaction effects,[7] in which rapid activated oxygen and/or electron transfer between metal and support could be involved.[8] Such metal–support interaction was reported to increase the catalytic activity and selectivity of Pt.[9] Thus, the design of heterogeneous catalysts composed of ceria with Pt nanoparticles is of fundamental importance.

(1) To achieve high catalytic activity, the noble metal is usually prepared as nanoparticles while the metal supports are in the form of porous structures. Easy preparation methods and recyclable products are highly desirable. Noble metal/oxide catalysts are usually prepared through template-free methods, lacking precise control over the structure and morphology of the catalysts. Several novel methods have recently been reported to prepare noble metal/oxide catalysts with secondary nanostructures. Notably, Wang and co-workers reported a general method for the fabrication of mesoporous oxides loaded with noble metal nanoparticles by aerosol spraying and solvent-evaporation-induced assembly.[10] Zhang *et al.* designed an ingenious route to uniform pomegranate-like Pt@ceria nanospheres by a redox reaction in argon.[11] Yet it remains challenging to prepare well-controlled and uniform catalyst structures. Hard template methods could offer easy access to structures with well-defined pore architectures and high surface area, which are required for high catalytic performance.[12] For example, silica templates, such as SBA-15, SBA-16, MCM-48 and KIT-6, have been used for the synthesis of ceria nanomaterials.[13] However, several limitations of these approaches prevent them from having wider applications. Specifically:

(1) An additional step is required to dissolve the silica template after the formation of ceria;

(2) Hazardous chemicals are sometimes required, such as HF;

(3) Diverse structural defects form in ceria after the removal of the silica template, due to the oxygen linkage between silica and ceria.

On the other hand, organic templates have also been used for controlled synthesis of metal oxides and can be easily removed in the calcination process.[14] Especially interesting are polymer templates with relatively robust structures, providing excellent opportunities to prepare complex noble metal/metal

[a]*Guangdong Key Lab of Nano-Micro Materials Research, School of Chemical Biology and Biotechnology, Peking University Shenzhen Graduate School, Shenzhen, 518055, China. E-mail: jingzhao@pkusz.edu.cn*

[b]*Department of Materials Science & Engineering, South University of Science & Technology of China, Shenzhen, 518055, China. E-mail: liang.yy@sustc.edu.cn*

[c]*State Key Laboratory of Pharmaceutical Biotechnology, Institute of Chemistry and Biomedical Sciences, School of Life Sciences, Nanjing University, Nanjing, 210093, China*

† Electronic supplementary information (ESI) available. See DOI: 10.1039/c4ra08423c

hybrid structures with required properties.[15] Herein we present a feasible template-based approach for the fabrication of uniform, nanoporous Pt/CeO_2 hybrid microspheres (Fig. 1).

The advantages of polymer microsphere templates include well-controlled size and porosity and easily functionalized surfaces.[16] By removing the organic polymer templates, a hierarchical structure of fine Pt nanoparticles embedded on porous ceria microspheres was formed. These hybrid structures showed superior catalytic activity in the reduction of 4-nitrophenol (4-NP) to 4-aminophenol (4-AP)[17] compared to the Pt/ceria composite prepared without a template. The microsized catalyst was easily recycled with high recovery ratios and its activity was sustained after 5 cycles. This new approach to constructing metal nanoparticles embedded in porous metal oxide microspheres could pave a new way to synthesize efficient catalysts with good stability and easy recyclability.

Results and discussion

The preparation strategy of Pt/CeO_2 microspheres is shown in Fig. 1. Functionalized porous microspheres of poly(glycidyl methacrylate-*co*-ethylene glycol dimethacrylate), poly (GMA-*co*-EGDMA), were used as the sacrificial templates. The morphology and pore architecture of the obtained ceria microspheres could be simply adjusted by varying the polymer microspheres applied. Here, polymer microspheres with a diameter of 7.5 μm were chosen to construct the hybrid structure. This size offers easy recycling of the ceria hybrid materials in catalysis applications. SEM images of the polymer microsphere template were shown in Fig. S1,† suggesting a porous structure and uniform size distribution of the microspheres. Textural properties of the polymer microspheres are shown in Fig. S2.† The surface area of the polymer microspheres was 114 $m^2\ g^{-1}$, and the pore volume was 0.8 $cm^3\ g^{-1}$; this porous structure is suitable for adsorbance of metal ions and cerium gels. The surface of the monodisperse polymer microspheres was initially functionalized with quaternary ammonium groups *via* a ring-opening reaction of the epoxide groups of GMA with trimethylamine hydrochloride, and polymer microspheres terminated with large numbers of quaternary ammonium groups were obtained. FT-IR spectra of the polymer microspheres before and after reaction (Fig. S3†) confirmed the successful functionalization of the hard template. Then $PtCl_6^{2-}$ was adsorbed onto the surface of the quaternary ammonium group-terminated microspheres through an ion exchange with Cl^-. Cerium(III) nitrate was impregnated into the microspheres, followed by the addition of ethylene glycol as a reducing agent. The mixture was then heated at 60 °C in a drying oven, forming the ceria gel and generating Pt nanoparticles.[18] It was observed that the cerium gel was fully adsorbed into the pores of polymer microspheres during this process, and no nucleation of the CeO_2 nanoparticles outside the microspheres was detected (Fig. S4†). The Pt/polymer–ceria hybrid was then calcined in a muffle furnace at 600 °C for 12 h. During the calcination process, the ceria nanoparticles formed gradually and yielded microspheres loaded with Pt NPs. When the temperature reached 500 °C, the polymer hard template was removed and the residual ethylene glycol was burned off.[16]

The scanning electron microscopy (SEM) images (Fig. 2a and b) indicated that the resulting Pt/CeO_2 microspheres were uniform and monodisperse, with morphologies similar to their parent polymer microspheres. Particle size of the polymer microspheres changed from 7.5 μm to 4.0 μm after calcination when the ceria microspheres formed (Fig. S5†), which may be due to shrinkage of the skeleton and an increase in the density of ceria during the thermal treatment to remove the polymeric template. The transmission electron microscopy (TEM) image in Fig. 2c clearly reveals the porous structure of these

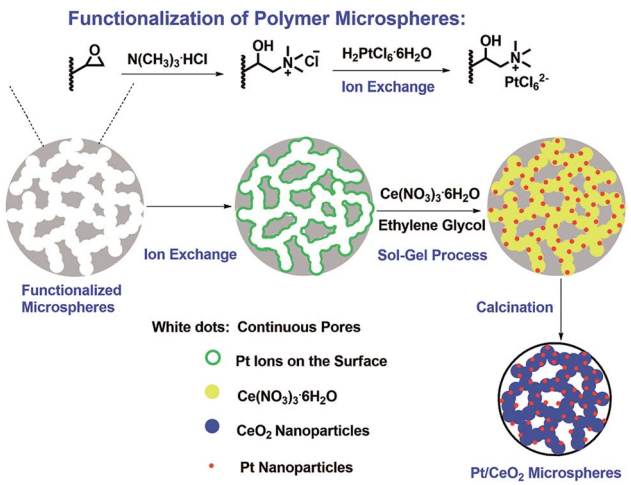

Fig. 1 Synthetic scheme of porous Pt/CeO_2 hybrid microspheres.

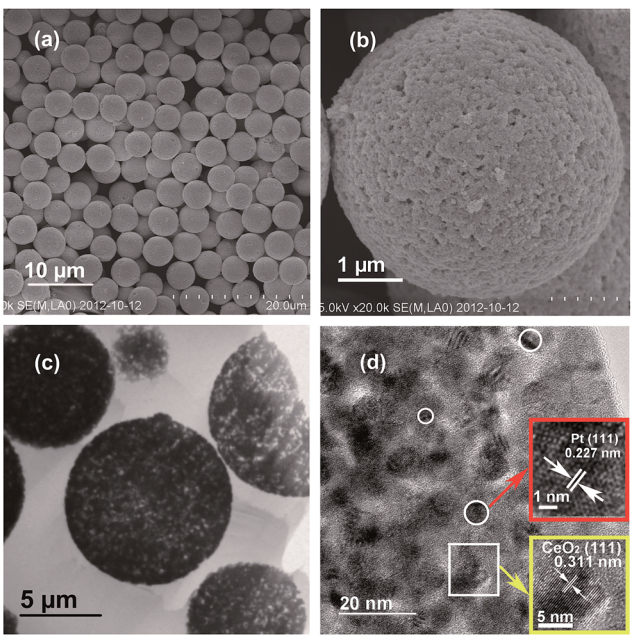

Fig. 2 SEM images and TEM images of Pt/CeO_2 microspheres: (a and b) SEM images of Pt/CeO_2 microspheres; (c) low resolution TEM image and (d) high resolution TEM image of Pt/CeO_2 microspheres (the bottom inset shows an enlarged image of a CeO_2 nanoparticle while the top inset shows an enlarged image of a Pt nanoparticle).

microspheres. CeO_2 thin slices with different diameters, shown in Fig. 2c, were acquired during the process of preparing TEM samples on a ion slicer as slices were cut through different sections of each Pt/CeO_2 microsphere. We observed dark spots distributed over the whole microspheres, which could correspond to crystalline CeO_2 and platinum nanoparticles (Fig. 2d). The major (111) crystalline planes with a 0.311 nm distance of CeO_2 were largely observed, and the particle size of these crystalline ceria nanoparticles was approximately 5–10 nm (Fig. 2d bottom inset). We also observed a small number of fine Pt nanoparticles (circles in Fig. 2d) with sizes of 2–5 nm in the high resolution TEM (HRTEM) images, and the lattice fringes correspond to the (111) crystalline plane of Pt as can be seen in the enlarged image in Fig. 2d (right middle inset) and S6.† The dark field scanning transmission electron microscopy image (STEM-DF) of the Pt/CeO_2 sample is shown in Fig. 3a, further revealing the hierarchic structures of the hybrid, with small dots approximately 1–2 nm in size embedded in the larger nanoparticles with sizes of 5–10 nm.

The element distribution obtained from the energy-dispersive X-ray spectroscopy (EDS) mapping indicated the uniform distribution of the Pt, Ce, O elements in the entire microsphere hybrid (Fig. 3b–d). The distribution of the small dots in STEM-DF correlated well with the Pt mapping, suggesting that the small dots could be Pt nanoparticles. Consistent with the HRTEM image, the size of the Pt nanoparticles was very small.

The XRD of Pt/CeO_2 microspheres showed sharp diffraction peaks corresponding to the face-centered cubic phase of ceria (JCPDS no. 34-0394), indicating good crystallinity (Fig. S7†). No obvious peaks of Pt nanoparticles were observed, partly due to their ultra-fine particle size. The N_2 adsorption–desorption isotherm of the Pt/CeO_2 microspheres had a hysteresis loop in the range of relative pressure $P/P_0 = 0.60$–0.99, indicating the mesoporous structure of the ceria microspheres (Fig. S8a†). The BJH pore size distribution of the Pt/CeO_2 microspheres (Fig. S8b†) exhibited a distribution between 1 and 50 nm. The BET surface area of the microspheres was 38 $m^2\ g^{-1}$, with an average pore diameter of 14 nm. The loading of Pt in the Pt/CeO_2 microspheres was determined by atomic absorption spectroscopy with an optical emission spectrometer, and was found to be 7.7 wt%. Pt/CeO_2 composite was also prepared *via* a similar but template-free method as a control for the Pt/CeO_2 microspheres. SEM images of the Pt/CeO_2 composite revealed its lack of structural regularity (Fig. S9†).

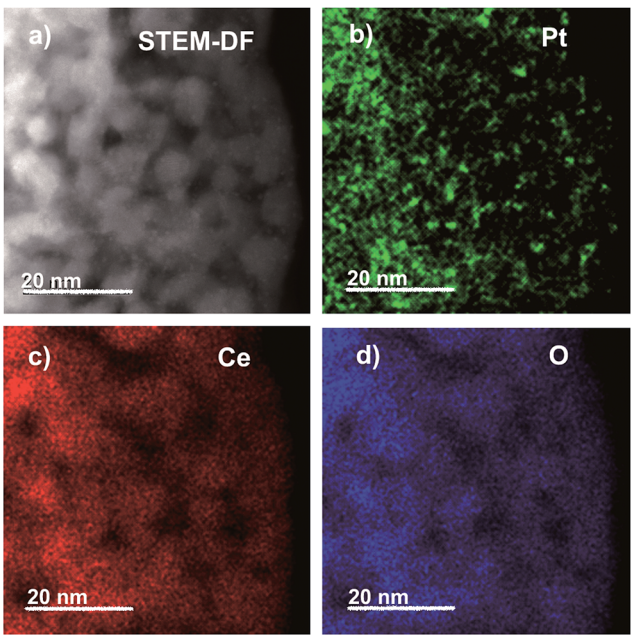

Fig. 3 (a) STEM-DF images of a detailed view of an individual Pt/CeO_2 microsphere and the corresponding elemental mappings of (b) Pt, (c) Ce and (d) O.

Catalytic study

The catalytic activities of the Pt/CeO_2 microspheres were evaluated by the catalytic reduction reaction of 4-NP to 4-AP, as shown in Fig. 4a. The absorption peak at 400 nm, corresponding to the formation of 4-nitrophenolate ion in alkaline

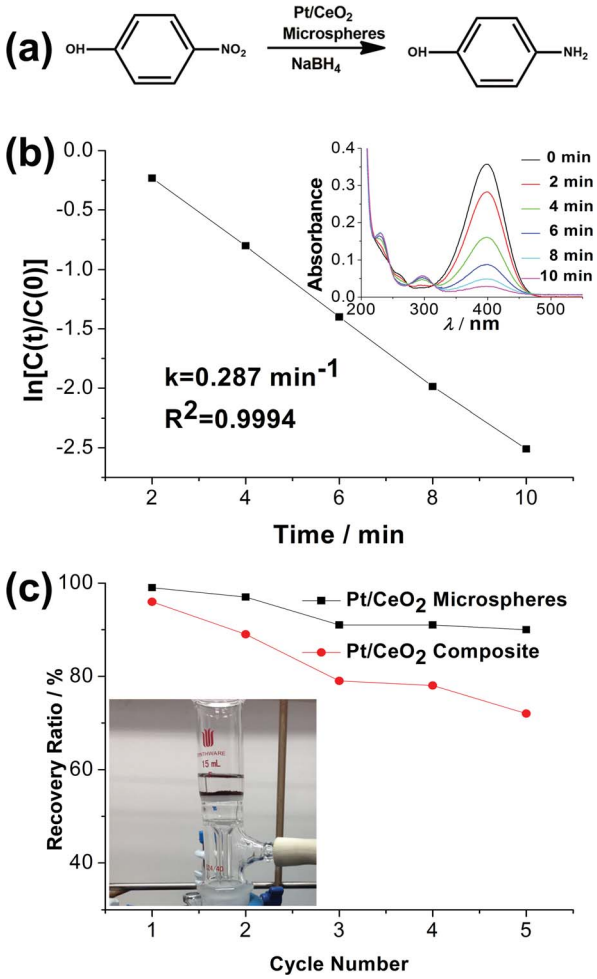

Fig. 4 (a) Reaction equation of the catalytic reduction of 4-NP to 4-AP; (b) plot of ln[C(t)/C(0)] against the reaction time by Pt/CeO_2 hybrid catalyst (right top inset: time-dependent absorption spectrum of the reaction solution); and (c) recovery ratio of Pt/CeO_2 microspheres and Pt/CeO_2 composite (5 cycles).

conditions,[17] remained unchanged in the absence of catalyst and gradually decreased in intensity after the addition of a very small amount of the Pt/CeO_2 microspheres. Concomitant increase of a new peak at 300 nm was observed, corresponding to the formation of 4-AP, the reduction product of 4-NP. Fig. 4b (right top inset) illustrates the absorption change of the above catalytic reduction process. The reaction rates were assumed to follow pseudo-first-order kinetics with respect to the reactants with a large excess of $NaBH_4$ relative to 4-NP. A linear relationship between $\ln[C(t)/C(0)]$ and reaction time was obtained, where $C(t)$ and $C(0)$ represent the concentration of 4-NP at time t and at the beginning of the reaction. The rate constants (k) were determined from the slopes and represented different reaction activities of the catalysts. The plot of $\ln[C(t)/C(0)]$ against the reaction time of Pt/CeO_2 microspheres is shown in Fig. 4b and the rate constant was calculated to be 0.287 min^{-1}.

With the presence of only CeO_2 microspheres or bare Pt nanoparticles, the model system showed little change in absorbance after the addition of $NaBH_4$, suggesting the low catalytic activity of the single component and the importance of the Pt/CeO_2 hybrid structure for catalysis (Fig. S10†). It should be noted that both the porous CeO_2 microspheres and Pt particles showed little absorption of the 4-NP during the measurements. This confirmed that the absorbance change in the Pt/CeO_2 system was caused by the reaction of 4-NP, instead of absorption by the porous microspheres. A control test was conducted with the Pt/CeO_2 composite under the same reaction conditions (Fig. S11†). The pseudo-first-order rate constant of the Pt/CeO_2 composite was 0.069 min^{-1}, which was much smaller than that of the Pt/CeO_2 microsphere catalyst (0.287 min^{-1}). The reaction time (90% of 4-NP consumed) of the Pt/CeO_2 composite catalyst (40 min) was approximately 4 times greater than that of the Pt/CeO_2 microspheres (11 min) under the same reaction conditions. The hierarchical porous CeO_2 microsphere support probably accounted for the higher catalytic activity of the Pt/CeO_2 microspheres compared to the structure-irregular composite materials. Pt nanoparticles were uniformly dispersed on the metal oxide support without obvious aggregation, which helped improve the catalytic activities of the Pt/CeO_2 hybrid catalyst in this diffusion-controlled reaction.

A recycling test was carried out to evaluate the reusability of the Pt/CeO_2 microspheres after 5 reaction cycles of the liquid phase catalytic reduction of 4-NP to 4-AP. The reaction time of each cycle was defined as the time (min) at which 90% of 4-NP was consumed, and these times are shown in Fig. S12.† The catalytic efficiencies of the Pt/CeO_2 microspheres remained relatively constant after 5 successive cycles. In the second cycle, activity dropped slightly and the reaction time changed from 11 min to 14 min. The reaction time was relatively well maintained, between 14 min and 16 min, in the following four cycles. Instability of $NaBH_4$ may affect the recyclability of the Pt/CeO_2 catalyst and a 10% weight loss of catalyst during the recovery process would also result in the decrease of catalytic activity after 5 cycles.[11] A study of the recovery ratio was also performed in the model reaction of 4-NP to 4-AP. The results shown in Fig. 4c demonstrated that the Pt/CeO_2 microspheres were easily recovered through centrifugation at 2000 rpm and the recovery ratio remained above 90% after 5 cycles, while the recovery ratio of the Pt/CeO_2 composite dropped to 72%. Additionally, the Pt/CeO_2 microspheres could be recycled through a sand core funnel, which is shown in Fig. 4c inset. Further, our catalyst survived after thermal treatment at 700 °C and even higher at 800 °C with no loss of catalytic activity in the model system (Fig. S13†). It is believed that the microsized and monodispersed structures of the Pt/CeO_2 hybrid improved the cycling ability of the catalyst.

With this general template-mediated method in hand, Au/CeO_2, Pd/CeO_2, Ag/CeO_2 and Cu/CeO_2 microspheres were synthesized through a similar approach to that of the Pt/CeO_2 microspheres. For the synthesis of Au and Pd nanoparticles, quaternary ammonium group-terminated polymer microspheres were used. Au nanoparticles were obtained *in situ* as the quaternary ammonium functional groups on the microspheres could reduce $AuCl_4^-$ during the calcination process. PdO nanoparticles deposited on CeO_2 microspheres were reduced to Pd nanoparticles using hydrazine hydrate as a reducing agent. Ag and Cu nanoparticles were developed from sulfonated microspheres (Scheme S14†). AgO nanoparticles decomposed at the calcination temperature and Ag nanoparticles formed. Hydrogen reduction was performed to guarantee the formation of Cu nanoparticles after calcination. SEM images of the various metal NPs/CeO_2 microspheres are shown in Fig. S15,† indicating that the as-prepared metal NP-loaded ceria microspheres possessed porous structures with uniform size distribution. EDS mappings of the Au/CeO_2 and Pd/CeO_2 microspheres are shown in Fig. S16 and S17 respectively,† indicating the uniform distribution of Au and Pd nanoparticles. Metal loadings of those metal NPs/CeO_2 microspheres are listed in Table S1.† Other metal oxide supports, such as ZrO_2, could be synthesized by a similar fabrication method.[19] As such, our approach could be extended to a wide range of noble metal/metal oxide hybrids with nanoporous and monodispersed structures.

Conclusions

In summary, we have presented a simple and general route for the fabrication of metal nanoparticles deposited on uniform and porous ceria microspheres by employing poly (GMA-*co*-EGDMA) microspheres as a hard template. The nanoporous, hierarchical and microsized Pt/CeO_2 hybrid structure exhibited high catalytic activity and good recycling stability, as well as easy recovery. This general synthetic method could be used to generate uniform and porous metal oxide microspheres embedded with metal nanoparticles, opening a door to the synthesis of advanced catalysts for various catalytic applications.

Experimental section

Chemicals and materials

The ceria precursor cerium(III) nitrate hexahydrate ($Ce(NO_3)_3 \cdot 6H_2O$) was purchased from Beijing Ouhe. Hydrochloroplatinic acid ($H_2PtCl_6 \cdot 6H_2O$), chloroauric acid tetrahydrate ($HAuCl_4 \cdot 4H_2O$),

palladium nitrate dehydrate ($Pd(NO_3)_2 \cdot nH_2O$) and trimethylamine hydrochloride ($N(CH_3)_3 \cdot 6HCl$) was purchased from Sinopharm Chemical Reagent Co., Ltd. Cupric nitrate ($Cu(NO_3)_2$) was purchased from Tianjin Damao. Silver nitrate ($AgNO_3$), sodium borohydride ($NaBH_4$) and 4-nitrophenol (4-NP) were supplied by Alfa Aesar. Sodium sulfite (Na_2SO_3) was purchased from Tianjin Zhiyuan. Porous poly-
(GMA-*co*-EGDMA) polymer microspheres were supplied by Nano-Micro Technology Company, China. Polyvinyl pyrrolidone (PVP) was purchased from Sigma Aldrich. Water was purified by distillation followed by deionization using ion exchange resins. All chemicals were analytical grade and used without further purification.

Characterization techniques

Powder X-ray diffraction (XRD) of Pt nanoparticles/CeO_2 microspheres was recorded using a Rigaku D/Max-2200 PC diffractometer in the diffraction angle range $2\theta = 10$–80° with Cu Kα radiation at 40 KV, 200 mA. The morphology and size of the microspheres were observed by field emission scanning electron microscope (FESEM) on a Hitachi S4800 scanning electron microscope (Japan). The transmission electron microscopy (TEM) was performed on a JEOL JEM-2100F field emission source transmission electron microscope operated at 200 kV and TEM-EDS X-ray mapping was conducted by using an IET X-max80 machine (Britain). N_2 adsorption–desorption isotherms, BET (Brunauer–Emmett–Teller) surface area, pore volume, and pore size of the microspheres were measured at liquid nitrogen temperature (−196 °C) on a Micromeritics Tristar II 3020 v1.03 analyzer (USA). Prior to the measurement, samples were subjected to a vacuum system, and then kept under vacuum at 120 °C for at least 12 h. UV absorption spectra of the catalytic reduction of 4-NP to 4-AP were measured ranging from 200 nm to 600 nm using a Shimadzu UV-2006 UV-Vis spectrophotometer (Japan). The particle size distribution was measured using a Multisizer 3 Coulter counter (Germany).

Procedure for the preparation of monodisperse porous ceria microspheres embedded with Pt nanoparticles

40 mL of 0.02 mol L^{-1} $PtCl_6^{2-}$ solution was added to a suspension of 5 g of quaternary ammonium group-terminated polymer microspheres dispersed in 200 mL distilled water. After stirring for 6 h at room temperature, the mixture was filtered through a sand core funnel and washed repeatedly with water. Then the microspheres were dried in an oven at 60 °C for 6 h. To a suspension of 1 g of microspheres adsorbed with platinum cations in 3 mL water, 2 g of $Ce(NO_3)_3 \cdot 6H_2O$ in 2 mL water was added, and 1 g of ethylene glycol was added as a reducing agent to obtain Pt nanoparticles. The mixed solution was transferred to an oven set at 60 °C and then heat-treated for 6 h. Finally, the obtained poly(GMA-*co*-EGDMA)/cerium microspheres with platinum cations or nanoparticles were calcined at 600 °C for 12 h.

Catalytic study

For the catalytic reduction of 4-NP, an aqueous solution of 4-NP (5 mM, 5 mL) was mixed with fresh aqueous $NaBH_4$ solution (0.4 M, 25 mL) in a three-necked round-bottom flask, and then 2 mL aqueous dispersion of Pt/CeO_2 microspheres (2.0 mg) was rapidly added with mechanical stirring at room temperature. The UV-visible absorption spectra of the reaction mixture were recorded to monitor the reaction progress. Catalytic activities of the catalysts were estimated by pseudo-first-order rate constants of the plot of $\ln[C(t)/C(0)]$ against the reaction time.

Recyclability test

In the recyclability test, 2 mg of the Pt/CeO_2 microspheres (Pt/CeO_2 composite) were dispersed in fresh aqueous $NaBH_4$ solution (0.4 M, 25 mL), and then an aqueous solution of 4-NP (5 mM, 5 mL) was added to the solution with mechanical stirring. The UV-visible absorption value for the peak at 400 nm was measured over the entire reaction every 2 minutes. After completion of the reaction, the microspheres were collected by centrifugation at 2000 rpm for 2 min and washed with water and alcohol. The catalysts were dried and reused directly without further treatment for another 4 cycles. Activities were evaluated by reaction time.

Acknowledgements

This work is financially supported by grants from the National Basic Research Program of China (2010CB923303), the National High Technology Research and Development Program of China (2014AA020512). J. Z. thanks the Shenzhen Government (SW201110018, JC201104210113A, KQC201105310016A) for support.1).

Notes and references

1 (*a*) S. J. Tauster, S. C. Fung and R. L. Garten, *J. Am. Chem. Soc.*, 1978, **100**, 170–175; (*b*) G. Dutta, U. V. Waghmare, T. Baidya and M. S. Hegde, *Chem. Mater.*, 2007, **19**, 6430–6436.
2 C. Chen, C. Nan, D. Wang, Q. Su, H. Duan, X. Liu, L. Zhang, D. Chu, W. Song, Q. Peng and Y. Li, *Angew. Chem., Int. Ed*, 2011, **50**, 3725–3729.
3 C. Hardacre, R. M. Ormerod and R. M. Lambert, *J. Phys. Chem.*, 1994, **98**, 10901–10905.
4 (*a*) M. Abid and R. Touroude, *Catal. Lett.*, 2000, **69**, 139–144; (*b*) J. Silvestre-Albero, F. Rodríguez-Reinoso and A. Sepúlveda-Escribano, *J. Catal.*, 2002, **210**, 127–136.
5 (*a*) Q. Fu, H. Saltsburg and M. Flytzani-Stephanopoulos, *Science*, 2003, **301**, 935–938; (*b*) D. Tibiletti, A. Goguet, F. C. Meunier, J. P. Breen and R. Burch, *Chem. Commun.*, 2004, 1636–1637.
6 (*a*) C. T. Campbell and C. H. F. Peden, *Science*, 2005, **309**, 713–714; (*b*) F. Esch, S. Fabris, L. Zhou, T. Montini, C. Africh, P. Fornasiero, G. Comelli and R. Rosei, *Science*, 2005, **309**, 752–755.

7 (*a*) J. A. Farmer and C. T. Campbell, *Science*, 2010, **329**, 933–936; (*b*) S. Bernal, J. Kaspar and A. Trovarelli, *Catal. Today*, 1999, **50**, 173–173.

8 (*a*) G. N. Vayssilov, Y. Lykhach, A. Migani, T. Staudt, G. P. Petrova, N. Tsud, T. Skála, A. Bruix, F. Illas, K. C. Prince, V. R. Matolín, K. M. Neyman and J. Libuda, *Nat. Mater.*, 2011, **10**, 310–315; (*b*) A. Caballero, J. P. Holgado, V. M. Gonzalez-delaCruz, S. E. Habas, T. Herranz and M. Salmeron, *Chem. Commun.*, 2010, **46**, 1097–1099; (*c*) S. Bernal, J. J. Calvino, M. A. Cauqui, J. M. Gatica, C. Larese, J. A. Pérez Omil and J. M. Pintado, *Catal. Today*, 1999, **50**, 175–206.

9 M. A. Vannice, C. C. Twu and S. H. Moon, *J. Catal.*, 1983, **79**, 70–80.

10 Z. Jin, M. Xiao, Z. Bao, P. Wang and J. Wang, *Angew. Chem., Int. Ed.*, 2012, **51**, 6406–6410.

11 X. Wang, D. Liu, S. Song and H. Zhang, *J. Am. Chem. Soc.*, 2013, **135**, 15864–15872.

12 (*a*) X. Ji, K. T. Lee and L. F. Nazar, *Nat. Mater.*, 2009, **8**, 500–506; (*b*) P. G. Bruce, B. Scrosati and J. M. Tarascon, *Angew. Chem., Int. Ed*, 2008, **47**, 2930–2946; (*c*) C. Y. Ma, Z. Mu, J. J. Li, Y. G. Jin, J. Cheng, G. Q. Lu, Z. P. Hao and S. Z. Qiao, *J. Am. Chem. Soc.*, 2010, **132**, 2608–2613.

13 (*a*) F. Kleitz, S. H. Choi and R. Ryoo, *Chem. Commun.*, 2003, 2136–2137; (*b*) B. Tian, X. Liu, H. Yang, S. Xie, C. Yu, B. Tu and D. Zhao, *Adv. Mater.*, 2003, **15**, 1370–1374; (*c*) W. Yue and W. Zhou, *J. Mater. Chem.*, 2007, **17**, 4947–4952; (*d*) F. Ying, S. Wang, C.-T. Au and S.-Y. Lai, *Microporous Mesoporous Mater.*, 2011, **142**, 308–315.

14 (*a*) M. Agrawal, S. Gupta, A. Pich, N. E. Zafeiropoulos and M. Stamm, *Chem. Mater.*, 2009, **21**, 5343–5348; (*b*) M. Sanlés-Sobrido, M. Pérez-Lorenzo, B. Rodríguez-González, V. Salgueiriño and M. A. Correa-Duarte, *Angew. Chem., Int. Ed.*, 2012, **51**, 3877–3882; (*c*) Y. Chen and J. Lu, *J. Porous Mater.*, 2012, **19**, 289–294.

15 K. Yoon, Y. Yang, P. Lu, D. Wan, H. C. Peng, K. Stamm Masias, P. T. Fanson, C. T. Campbell and Y. Xia, *Angew. Chem., Int. Ed.*, 2012, **124**, 9681–9684.

16 (*a*) J. He, C. Yang, X. Xiong and B. Jiang, *J. Polym. Sci., Part A: Polym. Chem.*, 2012, **50**, 2889–2897; (*b*) Y. Wang, J. He, J. Chen, L. Ren, B. Jiang and J. Zhao, *ACS Appl. Mater. Interfaces*, 2012, **4**, 2735–2742.

17 N. Pradhan, A. Pal and T. Pal, *Colloids Surf., A*, 2002, **196**, 247–257.

18 G. D. Moon and U. Jeong, *Chem. Mater.*, 2008, **20**, 3003–3007.

19 J. He, J. Chen, L. Ren, Y. Wang, C. Teng, M. Hong, J. Zhao and B. Jiang, *ACS Appl. Mater. Interfaces*, 2014, **6**, 2718–2725.